

Triplet excitations in low- H_c spin-gap systems KCuCl_3 and TlCuCl_3 : An inelastic neutron scattering study

N. Cavadini,¹ Ch. Rüegg,¹ A. Furrer,¹ H.-U. Güdel,² K. Krämer,² H. Mutka,³ and P. Vorderwisch⁴

¹Laboratory for Neutron Scattering, ETH Zürich & Paul Scherrer Institut, CH-5232 Villigen PSI, Switzerland

²Department for Chemistry and Biochemistry, Universität Bern, CH-3000 Bern 9, Switzerland

³Institut Laue-Langevin, B.P. 156, F-38042 Grenoble Cedex 9, France

⁴BENSC, Hahn-Meitner-Institut, D-14109 Berlin Wannsee, Germany

(Received 22 October 2001; published 26 March 2002)

Elementary excitations in valence bond magnets have a finite spin gap $\Delta = g\mu_B H_c$ to well-defined triplet states. The degeneracy of the triplet states is lifted in the presence of an external field, according to the Zeeman interaction term. The energy and intensity of the excitation spectra in $S=1/2$ valence bond KCuCl_3 and TlCuCl_3 are investigated by inelastic neutron scattering at finite external fields. Experimental observations along representative directions of reciprocal space are addressed up to $H/H_c \sim 0.6$ and $H/H_c \sim 0.9$, respectively. A comprehensive analysis of the split Zeeman modes is reported, which shows excellent agreement with first principles. The obtained results extend former characterizations at $H=0$ and are of importance in the context of the field-driven quantum criticality realized in the sister compounds KCuCl_3 and TlCuCl_3 .

DOI: 10.1103/PhysRevB.65.132415

PACS number(s): 75.10.-b, 71.70.-d, 78.70.-g

Increasing efforts were recently devoted to KCuCl_3 and TlCuCl_3 because of the experimental observation of a quantum spin gap by susceptibility and high-field magnetization investigations; see Refs. 1,2 and Ref. 3, respectively. The magnetic properties of the title compounds relate to $S=1/2$ interactions between the Cu^{2+} sites. A first description in terms of $S=1/2$ spin ladder interactions was motivated by structural considerations, which tentatively identified the relevant quantum units with double-spin chains running along the a direction of the monoclinic unit cell; see Ref. 1. This identification was invalidated after the complete exploration of the elementary excitations by inelastic neutron scattering on single crystals, which revealed energy dispersion of the excited triplet states $\epsilon(q)$ along each direction of reciprocal space. The microscopic description of the magnetic interactions within an antiferromagnetic (AF) Heisenberg model in the three-dimensional (3D) valence bond limit is summarized in Refs. 4–6 and references therein. The 3D interactions unambiguously determined by inelastic neutron investigations reveal an unexpected quantum regime (cf. Ref. 1) which is of particular interest at finite external fields. The reduction and eventual suppression of the spin excitation gap Δ at the critical field $H_c = \Delta/g\mu_B$ drives the quantum phase transition which separates at “ $T=0$ ” the quantum-disordered singlet ground state ($H < H_c$) from the field-induced 3D ordered ground state ($H > H_c$). The critical fields reported from static measurements in KCuCl_3 and TlCuCl_3 correspond to ~ 23 T and ~ 6 T, respectively, as summarized in Refs. 7–9.

The field-induced quantum phase transition in valence bond magnets as above is ascribed to the universality class of Bose-Einstein condensation; see Refs. 10 and 11. Applying a mapping of the triplet states to a diluted Bose gas, the relevant thermodynamic quantities are borrowed from the rich literature on the subject—a scenario successfully invoked in application to the present compounds in Ref. 12. Markedly less confidence can be claimed in the characterization of the

elementary excitations. Suitable systems with experimentally accessible H_c are rare and comprehensive inelastic neutron scattering studies of reference 3D valence bond magnets are to date lacking. In the following, detailed neutron spectra of the spin dynamics observed at finite fields in $S=1/2$ KCuCl_3 and TlCuCl_3 single crystals are presented, partly relieving the aforementioned unbalance.

As will be demonstrated, relevant aspects of the quantum phase transition occurring at H_c are inferred from the field dependence of the excitations at $H < H_c$, to which our concerns are devoted in the present study. The method and salient results at fixed $T=1.5$ K are summarized as follows: The Zeeman splitting of the triplet states $|1 S^z\rangle, S^z = \{0, \pm 1\}$ is investigated up to $H/H_c \sim 0.6$ in KCuCl_3 and $H/H_c \sim 0.9$ in TlCuCl_3 . The relative energy separation and intensity distribution observed at finite fields reflect the expectations from the elementary Zeeman interaction term to be introduced in Eq. (1), showing no intrinsic dependence on the wave vector along the complete directions investigated. Progressive linear energy splitting is reported up to the maximum field discussed. These results support the picture of soft Zeeman modes driving the quantum phase transition at the 3D AF zone center, determined by the common interaction scheme in both KCuCl_3 and TlCuCl_3 from Refs. 5 and 6. For TlCuCl_3 recent *elastic* neutron scattering experiments at $H > H_c$ evidenced the appearance of magnetic Bragg reflections in agreement with the above; see Ref. 13. Present *inelastic* neutron investigations illustrate the experimental realization of first principles on the whole spectral range of a family of 3D valence bond magnets. They further introduce the framework of the spin dynamics at $H > H_c$ to be described elsewhere; see Ref. 14.

Measurements were performed on the cold neutron spectrometers V2 at the Hahn-Meitner-Institut (HMI), Berlin and IN14 at the Institut Laue-Langevin (ILL), Grenoble. Both instruments were operated at fixed final energy $E_f = 4.7$ meV with a berillium filter in front of the analyzer.

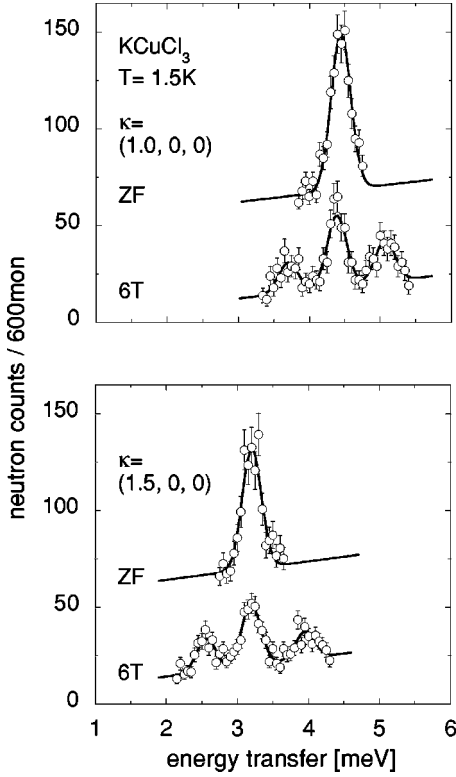


FIG. 1. Typical neutron profiles measured in KCuCl_3 at $T = 1.5$ K for zero field (ZF) and $H = 6$ T, wave vectors $\kappa = (1.0, 0, 0)$ and $\kappa = (1.5, 0, 0)$ [r.l.u.] as indicated, IN14. Profiles are vertically displaced by 50 units for convenience; instrumental parameters and fits to the observed energy separation and intensity distribution between the split triplet modes are discussed in the text.

Standard focusing conditions with open collimation after the sample yielded the common elastic energy resolution ~ 0.2 meV, as determined from the full width at half maximum (FWHM) of the incoherent line. The sample environment at $T = 1.5$ K with a vertical external field was adopted. Preparation and characterization of the single crystals aligned for scattering in the a^*c^* plane are described in our earlier investigations at zero field; see Ref. 6 and references therein. With respect to the topics of our concern, measurements up to $H = 14$ T ($H/H_c \sim 0.6$) in KCuCl_3 and up to $H = 5.5$ T ($H/H_c \sim 0.9$) in TlCuCl_3 are presented here. Slight deviations from $g = 2$ affect the quantitative, but not qualitative behavior of the magnetic properties of the $S = 1/2$ K/TlCuCl_3 family as addressed in Refs. 1–3. For the present investigation $H \parallel b^*$ is set as surveyed in a recent study of the field-induced ordering in TlCuCl_3 by elastic neutron scattering.¹³

In the following we quantitatively motivate the main conclusions already anticipated. In Fig. 1 neutron profiles at different wave vectors along the double-chain units demonstrate the characteristic energy and intensity response of the magnetic excited states observed at $T = 1.5$ K under finite fields. Well-defined triplet modes are reported up to the maximum H/H_c ratio addressed in both KCuCl_3 and TlCuCl_3 compounds. The investigations in the a^*c^* plane comprise the $[x, 0, 0]$ direction for the former and $[x, 0, 0]$, $[-x, 0, 2x + 1]$ directions for the latter. In Fig. 2 (top panel) the energy

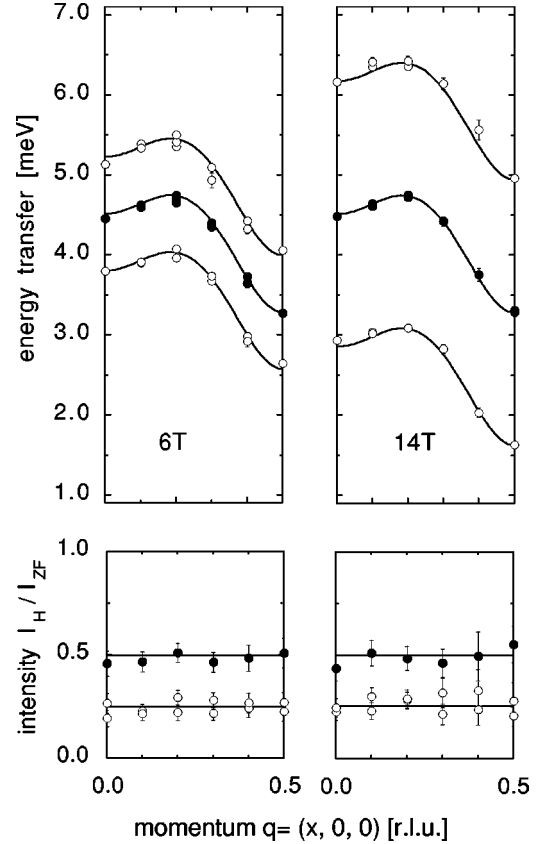


FIG. 2. Observed energy separation (top) and intensity distribution (bottom) between the triplet modes measured along $[x, 0, 0]$ in KCuCl_3 at $T = 1.5$ K. Data in the reduced zone representation correspond to experiments performed at $H = 6$ T (left) and $H = 14$ T (right). Solid and open circles denote the $S^z = 0$ and $S^z = \pm 1$ states, respectively and solid lines refer to the model expectations detailed in the text.

dispersion of the Zeeman-split modes is summarized in KCuCl_3 at $H = 6$ T and $H = 14$ T along the irreducible portion of the $[x, 0, 0]$ direction as indicated. Solid lines represent the calculated zero-field dispersion $\epsilon(q)$ from Refs. 5 and 6, split according to the Zeeman interaction term

$$\hat{H}^z = -g\mu_B S \cdot \mathcal{H}, \quad \mathcal{H} = He^z, \quad (1)$$

yielding $\{0, \mp (g/2)0.116\}$ meV/T for the $S^z = \{0, \pm 1\}$ states, respectively. Following the usual notation, g denotes the Landé factor of the triplet states, μ_B Bohr's magneton, and e^z the unit vector along the quantization axis in spin space. The symbols in Fig. 2 are extracted from fits to the observed neutron spectra explained below. At each wave vector, the global fit procedure consists of a common background on bottom of one degenerate mode in zero field and three split modes at finite fields, as exemplified in Fig. 1. The neutron spectra collected in zero field under the same instrumental conditions provide reference quantities for the subsequent evaluation of the energy and intensity dependence. We concentrate in the following on the relative change imposed by Eq. (1) at each investigated wave vector. The results summarized in Fig. 2 (top panel) demonstrate the characteristic observations throughout reciprocal space and indicate within

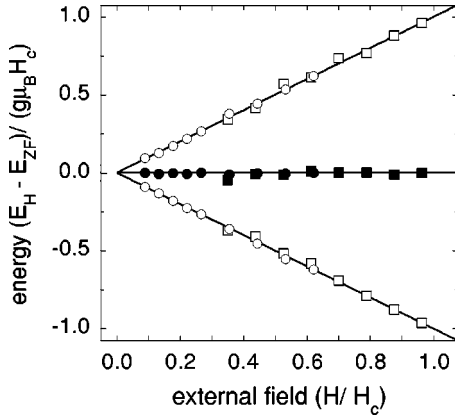


FIG. 3. Summary of the progressive Zeeman splitting of the triplet modes observed in KCuCl_3 (circles) and TiCuCl_3 (squares) at $T=1.5$ K up to 14 T and 5.5 T, respectively. The energy separation is compared to the model expectations in the same representation as Fig. 2; data sets and scaled units are explained in the text.

experimental accuracy that the energy of the $S^z=0$ mode remains unaffected by the applied field (solid circles) and that the energy of the $S^z=\pm 1$ modes closely follows the Zeeman term (open circles). The same quantitative conclusions extend to TiCuCl_3 measured at $H=5.5$ T (not shown in the figure). Overall refinement of the g factors as the only free parameter in the model expectation from Eq. (1) yields $g=2.04(2)$ and $g=2.10(4)$ for KCuCl_3 and TiCuCl_3 , respectively. These values compare well to the static measurements in Refs. 3 and 7–9.

Linear energy splitting of the Zeeman modes in both KCuCl_3 and TiCuCl_3 is observed up to the maximum field addressed. In Fig. 3 data to be described below are presented in a doubly reduced scale, for which normalized $(g/2)H_c$ at $T=1.5$ K is fixed at 23 T and 6 T, respectively, with the Landé factor g as determined above. Symbols summarize the overall refinements at $H=6$ T, $H=14$ T (in KCuCl_3), and $H=5.5$ T (in TiCuCl_3) along the directions previously discussed, completed by additional measurements at intermediate fields restricted to well-resolved points of reciprocal space. These correspond to $\kappa=(0.7,0,0)$, $\kappa=(1.2,0,0)$, and $\kappa=(-0.5,0,2)$ [r.l.u.], respectively. Some neutron profiles of the progressive splitting from the former were previously reported in Ref. 15. The totality of the obtained results supports the picture of soft Zeeman modes by linear extrapolation at the 3D AF zone center $\kappa=(0,0,1)$ [r.l.u.] and equivalent points; see also Ref. 13. We remark, however, that the flank of the incoherent line prevents the full determination of the soft mode in TiCuCl_3 at $\kappa=(0,0,1)$ [r.l.u.] due to the finite resolution. Here the observed $S^z=\{0,-1\}$ states at $H=5.5$ T compare well with the overall refinements in Fig. 3 as explained. Spin resonance measurements also reveal the progressive linear reduction of the spin gap at finite fields. Albeit lacking direct identification in reciprocal space, experimental conclusions from the title compounds are in agreement with Fig. 3; see Ref. 16.

The size of the Zeeman splitting from Eq. (1) is comparable to the bandwidth of the excitations; see Fig. 2 (upper panel). The simple results obtained from the energy analysis

indicate that the Zeeman regime is not perturbative but exact—in contrast to similar investigations from $S=1$ Haldane compounds, where single-ion anisotropies strongly affect the experimental observations; see, for example, Refs. 17–19. We express this evidence through the elementary commutation relation

$$[\hat{H}^0 + \hat{H}^1 + \dots, \hat{H}^z] = 0, \quad (2)$$

where $\hat{H}^0 + \hat{H}^1 + \dots$ describes the valence bond expansion of the AF Heisenberg interaction in Refs. 5 and 6 and \hat{H}^z the Zeeman term from Eq. (1). The above relation implies the retention of the singlet-triplet symmetry of the spin states in the whole reciprocal space. Transition matrix elements are accordingly expected to reflect the isotropic spectral weight in the three fluctuation modes S^{xx} , S^{yy} , and S^{zz} , which enter the energy-integrated neutron cross section after

$$\frac{d\sigma}{d\Omega} \sim |f(\kappa)|^2 \sum_{\alpha\beta} \left(\delta^{\alpha\beta} - \frac{\kappa^\alpha \kappa^\beta}{\kappa^2} \right) S^{\alpha\beta}(\kappa), \quad (3)$$

where $\kappa=q+\tau$ is the scattering wave vector in the usual notation, $f(\kappa)$ the magnetic form factor of the Cu^{2+} ion, and $\alpha, \beta = \{x, y, z\}$ the spin component. The quantization axis z from Eq. (1) is out of the scattering plane, according to the experimental setup. Under the mentioned expectations, relative contributions to total intensity from the longitudinal spin fluctuation S^{zz} and from the transverse spin fluctuations S^{xx}, S^{yy} reduce after Eq. (3) to 1/2 and 1/4, 1/4, respectively. To leading order, these weights map to the $S^z=0$ and $S^z=\pm 1$ states at finite fields and are thus separately accessible from the observed neutron spectra. In Fig. 2 (bottom panel), the ratio of the energy-integrated intensities between the split modes is presented, where the mean value is given for common points in the irreducible representation. Within experimental accuracy, overall good agreement with the above expectations is reported, bearing in particular no significant dependence on the wave vector. The results presented clearly locate the title compounds in the criticality class of 3D AF Heisenberg magnets. Subtle distinctions between different spin models are often unimportant for zero-field and modest field properties but become of crucial importance around the quantum critical point; see, for example, Refs. 20 and 21. Relevant contributions to the understanding of the microscopic properties of elementary triplet modes are available from inelastic neutron scattering in the dimer phase of $S=1/2$ CuGeO_3 ; see Refs. 22–24. These provide dynamic insights in a large H/H_c range, comprising the high-field phase of a spin-Peierls compound in Ref. 24. However, the soft Zeeman mode abruptly collapses at $H/H_c \sim 0.84$ without extrapolating to 1, as explained by spin-Peierls theories (compare Fig. 3). The high-field phase bears accordingly distinct features, successfully addressed in Ref. 25 and references therein. The intrinsic coupling to the lattice degrees of freedom and the low-dimensional interaction scheme illustrate conditions of undoubted interest, which, however, cannot be considered prototypical for the quantum critical properties realized in the 3D valence bond K/TiCuCl_3 family. The advantageous (H, T) experimental range promotes the latter as

appealing testing ground for novel theories on its own right. To our knowledge, other notable representatives of field-induced magnetic ordering in the valence bond limit are investigated by inelastic neutron scattering in Refs. 26 and 27 and references therein. A random phase approximation theory self-consistently accounting for the spin dynamics at finite fields $H < H_c$ and finite temperatures is elaborated in Ref. 28.

We finally comment in the context of the (inappropriate) 1D ladderlike description of the title compounds, as already addressed in the beginning. Isolated $S=1/2$ ladder units in external fields are expected to enter an incommensurate (IC) magnetic phase at $H > H_c$, described by $\delta q = m(H)/2$, where $0 \leq m(H) \leq 1$ denotes the normalized field-induced magnetization per spin site.²⁰ Calculation of the dynamic structure factors indicates that the IC soft modes occur for transverse spin correlations at $q=0.5$ and for longitudinal spin correlations at $q=0$ along the ladder direction.^{10,20} From the present measurements, precursors of putative incommensurate energy shifts either in KCuCl_3 or TlCuCl_3 are not observed within experimental accuracy. Moreover, profiles of the separate transverse and longitudinal fluctuations at finite fields turn out to be comparable throughout the ladderlike direction; see also Fig. 1. The above facts further underline the 3D valence bond description of the title compounds. In TlCuCl_3 , recent elastic neutron measurements at $H > H_c$ evidence the progressive emergence of field-induced magnetic Bragg reflections in correspondence to the commensurate minima of

the 3D energy dispersion.¹³ These findings are in full agreement with the homogeneous threefold Zeeman splitting across the zero-field dispersion $\epsilon(q)$ presented in Figs. 1–3 and commented on in the text.

To conclude, a comprehensive study of the excited triplet states in $S=1/2$ KCuCl_3 and TlCuCl_3 was presented by means of inelastic neutron scattering at finite fields. Inclusion of the Zeeman interaction term from Eq. (1) in the valence bond model description excellently reproduces the experimental observations reported at $T=1.5$ K for different H/H_c ratios up to ~ 0.9 . The results represent major achievements from the experimental point of view, which corroborate the characterization of KCuCl_3 and TlCuCl_3 as reference quantum magnets of 3D valence bond nature and which make legitimate the Heisenberg description of their magnetic interactions. The evidenced behavior is of importance for a microscopic understanding of the field-induced quantum phase transition, as discussed. For TlCuCl_3 , first studies by inelastic neutron scattering in the ordered state at $H > H_c$ are anticipated. In this respect, the severe lack of theoretical expectations regarding the spin dynamics is stressed.

Fruitful discussions with B. Braun, H.-J. Mikeska, and B. Normand are appreciated. The support of M. Meissner and H. Schneider during the V2 measurement and of F. Thomas during the IN14 measurement is gratefully acknowledged. This work was financially supported by the Swiss National Science Foundation.

-
- ¹H. Tanaka, K. Takatsu, W. Shiramura, and T. Ono, *J. Phys. Soc. Jpn.* **65**, 1945 (1996).
²K. Takatsu, W. Shiramura, and H. Tanaka, *J. Phys. Soc. Jpn.* **66**, 1611 (1997).
³W. Shiramura, K. Takatsu, H. Tanaka, K. Kamishima, M. Takahashi, H. Mitamura, and T. Goto, *J. Phys. Soc. Jpn.* **66**, 1900 (1997).
⁴T. Kato, A. Oosawa, K. Takatsu, H. Tanaka, W. Shiramura, K. Nakajima, and K. Kakurai, *J. Phys. Chem. Solids* **60**, 1125 (1999).
⁵N. Cavadini, G. Heigold, W. Henggeler, A. Furrer, H.U. Gudel, K. Kramer, and H. Mutka, *J. Phys.: Condens. Matter* **12**, 5463 (2000).
⁶N. Cavadini, G. Heigold, W. Henggeler, A. Furrer, H.U. Gudel, K. Kramer, and H. Mutka, *Phys. Rev. B* **63**, 172414 (2001).
⁷A. Oosawa, M. Ishii, and H. Tanaka, *J. Phys.: Condens. Matter* **11**, 265 (1999).
⁸A. Oosawa, H. Tanaka, T. Takamasu, H. Abe, N. Tsujii, and G. Kido, *Physica B* **294-295**, 34 (2001).
⁹A. Oosawa, H. Aruga Katori, and H. Tanaka, *Phys. Rev. B* **63**, 134416 (2001).
¹⁰T. Giamarchi and A.M. Tsvelik, *Phys. Rev. B* **59**, 11 398 (1999).
¹¹S. Wessel and S. Haas, *Phys. Rev. B* **62**, 316 (2000).
¹²T. Nikuni, M. Oshikawa, A. Oosawa, and H. Tanaka, *Phys. Rev. Lett.* **84**, 5868 (2000).
¹³H. Tanaka, A. Oosawa, T. Kato, H. Uekusa, Y. Ohashi, K. Kakurai, and A. Hoser, *J. Phys. Soc. Jpn.* **70**, 939 (2001).
¹⁴Ch. Ruegg, N. Cavadini, A. Furrer, H.U. Gudel, K. Kramer, H. Mutka, and P. Vorderwisch, *Appl. Phys. A* (to be published).
¹⁵N. Cavadini, W. Henggeler, A. Furrer, H.U. Gudel, K. Kramer, and H. Mutka, *Eur. Phys. J. B* **7**, 519 (1999).
¹⁶K. Takatsu, W. Shiramura, H. Tanaka, T. Kambe, H. Nojiri, and M. Motokawa, *J. Magn. Magn. Mater.* **177-181**, 697 (1998).
¹⁷L.P. Regnault, I. Zaliznyak, J.P. Renard, and C. Vettier, *Phys. Rev. B* **50**, 9174 (1994).
¹⁸A. Zheludev, Y. Chen, C.L. Broholm, Z. Honda, and K. Katsumata, *Phys. Rev. B* **63**, 104410 (2001).
¹⁹A. Zheludev, Z. Honda, Y. Chen, C.L. Broholm, K. Katsumata, and S.M. Shapiro, cond-mat/0107416 (unpublished).
²⁰R. Chitra and T. Giamarchi, *Phys. Rev. B* **55**, 5816 (1997).
²¹M. Usami and S.I. Suga, *Phys. Rev. B* **58**, 14 401 (1998).
²²L.P. Regnault, M. Ain, B. Hennion, G. Dhalenne, and A. Revcolevschi, *Phys. Rev. B* **53**, 5579 (1996).
²³B. Grenier, L.P. Regnault, J.E. Lorenzo, J.P. Boucher, A. Hiess, G. Dhalenne, and A. Revcolevschi, *Phys. Rev. B* **62**, 12 206 (2000).
²⁴M. Enderle, H.M. Ronnow, D.F. McMorrow, L.P. Regnault, G. Dhalenne, A. Revcolevschi, P. Vorderwisch, H. Schneider, P. Smeibidl, and M. Meissner, *Phys. Rev. Lett.* **87**, 177203 (2001).
²⁵H.M. Ronnow, M. Enderle, D.F. McMorrow, L.P. Regnault, G. Dhalenne, A. Revcolevschi, A. Hoser, K. Prokes, P. Vorderwisch, and H. Schneider, *Phys. Rev. Lett.* **84**, 4469 (2000).
²⁶G. Xu, C. Broholm, D.H. Reich, and M.A. Adams, *Phys. Rev. Lett.* **84**, 4465 (2000).
²⁷B. Leuenberger, H.U. Gudel, R. Feile, and J.K. Kjems, *Phys. Rev. B* **31**, 597 (1985).
²⁸B. Leuenberger, *J. Phys. C* **19**, 4083 (1986).